Application of Recurrence Analysis to the period doubling cascade of a confined buoyant flow

IOP Conf. Series: Journal of Physics: Conf. Series **796** (2017) 012005 doi:10.1088/1742-6596/796/1/012005

Application of Recurrence Analysis to the period doubling cascade of a confined buoyant flow

D Angeli[1], M A Corticelli[2], A Fichera[3] and A Pagano [3]

[1] Dipartimento di Scienze e Metodi dell'Ingegneria, Università degli Studi di Modena e Reggio Emilia, Via Amendola 2, 42122 Reggio Emilia (Italy)
[2] Dipartimento di Ingegneria Enzo Ferrari, Università degli Studi di Modena e Reggio Emilia, Via Vivarelli 10, 41125 Modena (Italy)
[3] Dipartimento di Ingegneria Elettrica, Elettronica e Informatica, Università degli Studi di Catania, Viale Andrea Doria 6, 95125 Catania (Italy)

E-mail: diego.angeli@unimore.it

Abstract. Recurrence Analysis (RA) is a promising and flexible tool to identify the behaviour of nonlinear dynamical systems. The potentialities of such a technique are explored in the present work, for the study of transitions to chaos of buoyant flow in enclosures. The case of a hot cylindrical source centred in a square enclosure, is considered here, for which an extensive database of results has been collected in recent years. For a specific value of the system aspect ratio, a sequence of period doublings has been identified, leading to the onset of chaos. RA is applied here to analyse the different flow regimes along the route to chaos. The qualitative visual identification of patterns and the statistics given by the quantitative analysis suggest that this kind of tool is well suited to the study of transitional flows in thermo-fluid dynamics.

1. Introduction

Transition to chaos of thermal convection flows in enclosures is one of the most intriguing topics in the study of the onset of fluid turbulence [1]. Yet, the diversity of patterns and scenarios that could arise as a consequence of the interplay between the temperature and velocity fields is far from being completely unfolded. To this aim, different techniques can be employed for the analysis of nonlinear behaviours encountered throughout transition.

This study is concerned with the 2D numerical analysis of the dynamics of an air-filled isothermally cooled square cavity with a concentric horizontal cylindrical heat source, investigated with respect to the governing parameters of the non-dimensional description of the problem: the ratio between the cavity side length L and the minimum enclosure to cylinder gap width H, $A = L/H$, and the Rayleigh number Ra, for a fixed value of the Prandtl number $Pr = 0.7$. Recent results [2] showed that at least two distinct types of dynamics can be observed: (i) a thermal plume arising from the cylindrical source for low A-values ($A \leq 3.3$), and (ii) Rayleigh-Bénard-like cellular structures above the heat source for higher A-values ($A \geq 5$).

For the case $A = 2.5$ a thorough description was reported in [3–5] of the period-doubling route to chaos that the thermal plume undergoes for increasing Ra. Moreover, this bifurcation path was shown to be determined by the nonlinear interplay of two fundamental modes of the thermal fluid-dynamic system.

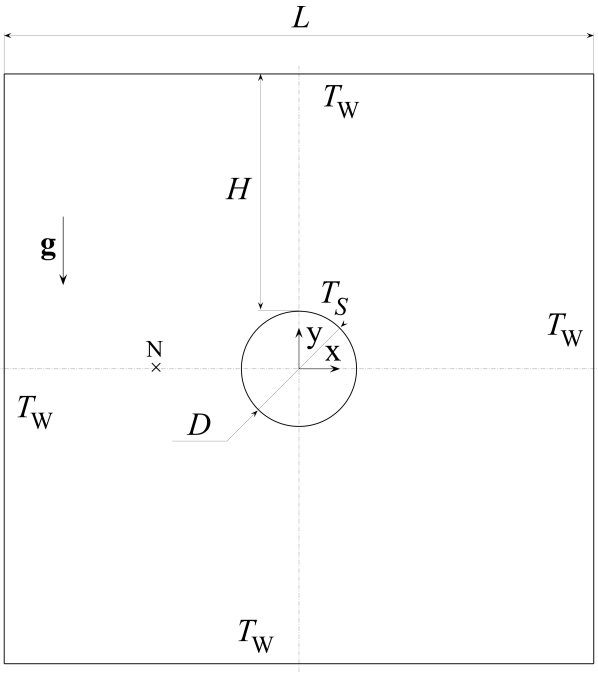

Figure 1. Schematic view of the system under consideration.

Substantially different is the mechanism involved for the case of the Rayleigh-Bénard cellular patterns that characterise the flow for $A = 5$. In fact, in this case the growth of Ra causes the progressive winding of the trajectory on an attractor resembling the features of a French horn, typical of the blue-sky catastrophe driving the transition from periodic dynamics to chaos in the Shilnikov's scenario [6]. Due to the complexity of this scenario and of the observed attractor, more sophisticated tools are required to identify unequivocally the system behaviour. With this respect, promising seems the adoption of the Recurrence Analysis (RA) [7].

With this purpose, the present study is devoted to test the tools made available by RA through their preliminary application to the description of the recurrent patterns observed in the dynamics of the swaying thermal plume for the case of sufficiently wide gap, at $A = 2.5$, so as to take advantage of the high level of refinement already reached in previous studies. In particular, the low order dynamics arising from the period-doubling cascade undergone by the basic periodic limit cycle will be followed by means of the Recurrence Plot of the intermediate regime solutions encountered on the way to chaos.

2. Problem statement

The problem is stated in terms of the incompressible Navier-Stokes formulation. The Oberbeck-Boussinesq approximation is enforced, all the fluid properties being consistently assumed as constant, apart from density in the buoyancy term.

The governing equations are tackled in their non-dimensional form. The gap between the top of the cylinder and the upper cavity wall is indicated in [8] as the most suitable scale length, $H_{ref} = H$. In fact, it reduces the dependence of the solution ranges on the aspect ratio, in particular, for what concerns the heat transfer rate and the first transitions between different regimes. Moreover, the region above the cylinder is subject to the maximum inverse thermal gradient, *i.e.* to the highest buoyancy force acting on the fluid system, and this is again related to the reference length H.

Temperature is non-dimensionalized according to a reference temperature T_{ref}, *i.e.* the

temperature difference between the cylinder and the cavity walls ($T_{ref} = T_S - T_W$), and the following velocity scale is chosen:

$$U_{ref} = \sqrt{g\beta T_{ref} H_{ref}} \tag{1}$$

where g denotes the gravitational acceleration and β is the thermal expansion coefficient of the fluid. Coherently, time is made dimensionless by choosing a reference time scale $t_{ref} = H/U_{ref}$. The continuity, momentum, and energy equations are then given the following form:

$$\nabla \cdot \mathbf{u} = \mathbf{0} \tag{2}$$

$$\frac{\partial \mathbf{u}}{\partial t} + \mathbf{u} \cdot \nabla \mathbf{u} = -\nabla p + \frac{Pr^{1/2}}{Ra^{1/2}} \nabla^2 \mathbf{u} + T\hat{\mathbf{g}} \tag{3}$$

$$\frac{\partial T}{\partial t} + \mathbf{u} \cdot \nabla T = \frac{1}{(RaPr)^{1/2}} \nabla^2 T \tag{4}$$

where t, $\mathbf{u}$, p and T represent the dimensionless time, velocity vector, pressure and temperature, respectively, and $\hat{\mathbf{g}}$ is the gravity unit vector. The Rayleigh and Prandtl numbers are defined as:

$$Ra = \frac{g\beta T_{ref} H_{ref}^3}{\nu\alpha} \tag{5}$$

$$Pr = \nu/\alpha \tag{6}$$

where ν and α represent the momentum and thermal diffusivity, respectively. A constant value $Pr = 0.7$ is assumed for air. With reference to figure 1, the following non-dimensional boundary conditions are imposed:

$$T = 0, \quad \mathbf{u} = \mathbf{0} \tag{7}$$

at the enclosure walls, and:

$$T = 1, \quad \mathbf{u} = \mathbf{0} \tag{8}$$

on the cylinder surface.

3. Numerical methods

The numerical technique adopted is based on a Finite Volume implementation of a second order Projection Method, following [9]. Time-discretizations of the conservation equations are performed according to a three-level scheme, which is fully implicit for the diffusive terms, and explicit Adams-Bashforth for the advective terms. Such a practice is second order accurate in time.

Spatial derivatives are approximated with second order central differences on staggered, non-uniform Cartesian grids. A direct resolution of the discrete momentum and energy equations at each time-step is made possible by means of Approximate Factorization, while the Poisson problem associated with the pressure-velocity coupling [9] is solved through a fast Poisson solver, based on Matrix Decomposition.

The 2D modelling of arbitrarily irregular boundaries on Cartesian grids is achieved thanks to the original scheme developed in [10]. The technique involves a local modification of the 5-point computational stencil where boundary segments intersect the stencil arms. The variables on the modified stencil are mapped on the global grid, by means of a linear operator determined by geometrical features and boundary conditions. The overall accuracy of the method is virtually preserved, as well as the computational efficiency of the Cartesian approach.

Details on the grid size, time step choice, initial conditions, are outlined in detail in [3], while a grid independency test for a periodic flow is reported in [8].

For the purposes of recurrence analyses, the time histories of dimensionless temperature T sampled at location N (as reported in figure 1) were considered. The simulated time series, originally collected with a fixed time step size $\Delta t = 8.25 \times 10^{-3}$, were resampled at a larger interval $\Delta t = 3.3 \times 10^{-2}$ in order to decrease the computational effort required by recurrence quantification.

4. Recurrence Analysis

Previous analyses of the simulated dynamics have been devoted to the topological description of the attractors in the state space spanned by the system variables, namely the dimensionless temperature and the horizontal and vertical components of the dimensionless velocity, sampled at specified points of the domain. The present study instead proposes a different approach aiming at characterising the observed recurrent behaviour of the state variables, which is a fundamental and typical property of nonlinear systems. In particular, the sequence of bifurcating attracting solutions arising for increasing Rayleigh number will be distinguished on the basis of the differences between the patterns in their recurrence plots.

The construction of the recurrence plot (RP) allows for the observation of the existence of recurrent states $\mathbf{x}_i$ of the attractor representation in an original m-dimensional phase space. The RP is a 2D representation space, with time spanning both axes, defined as [7]:

$$R_{i,j} = \Theta\left(\varepsilon - \|\mathbf{x}_i - \mathbf{x}_j\|\right), \, \mathbf{x}_i, \mathbf{x}_j \in \mathbb{R}_m, \, i, j = 1, \ldots, N \tag{9}$$

where N is the number of considered states $\mathbf{x}_i$, ε is a threshold distance defining the transvers dimension of the cylinder centred on the trajectory, $\|\cdot\|$ is the norm operator and $\Theta(\cdot)$ is the Heaviside function. This corresponds to representing the recurrence of states at two different time i and j with a black dot in the recurrence plot. The RP is symmetric with respect to the main diagonal, which corresponds to the line of identity (LOI). The application of statistical analyses of the distribution of points in the RP offers a variety of tools for the characterisation of the dynamics of the system under consideration. These tools are collectively addressed as recurrence quantification analysis (RQA) and will be synthetically described in the following.

The choice of the embedding dimension does not usually play a fundamental role and, hence, especially if the RP is used as the basis for RQA, it is often preferable simply to set it at 1, i.e. no embedding is required [11]. Similarly, also the time delay for the embedding is not determinant and, therefore, it can also be set at 1 [12]. It is worth observing that both the embedding dimension and the time delay are critical parameters in the application of traditional nonlinear tools based on attractor characterisation on phase space and, hence the analysis of the time series by means of RPs and RQA appears much simpler in this regard. Accordingly, in this study, both the embedding dimension m and the time delay τ have been set to 1.

Far more relevant is the choice of the threshold radius ε, both for the determination of the RP and for the application of the RQA tools; in fact, if the threshold is too small, only a limited number of recurrent state can be detected, whereas if it is too large false recurrence and even consecutive points of a trajectory will populate the RP. Various criteria have been proposed for an appropriate choice [7, 12, 13]. In particular, Webber and Zbilut [12] suggest to choose the radius threshold looking for a scaling region in the recurrence point density (RR).

Different topologies arise depending on the distribution of the black points in the RPs and, in fact, RPs allow for the identification of transitions and interrelations within the system dynamics. In fact, the topology of the RPs has been related [7] to the system dynamics. In particular, for the aims of the present study it is of interest the identification either of periodic behaviours, through the observation of diagonal lines in the RP, or of deterministic chaotic behaviours, which manifest themselves with isolated points close to periodic diagonal lines, as a consequence of the

existence of unstable periodic orbits. Also of interest is the observation of horizontal or vertical lines in the RP, as these are due to laminar states, i.e. states for which no appreciable change in the trajectory occurs within a certain time window. Beyond the interest of the present study, the study of Marwan et al. [7] also reports a detailed description of the RP topology of other classes of dynamical states, such as nonstationary, intermittent or strongly fluctuating phenomena.

As previously mentioned, the recurrence quantification analysis, RQA, represents a set of statistical tools for the synthetic description of a RP or for the comparison of RPs characteristic of different conditions [7, 12]. The following section reports a brief synthesis of these tools and their possible relation with the dynamics invariants typically used for the characterisation of nonlinear dynamics in phase space. The analytical definition of the reported parameters is omitted for brevity and can be found in the reported literature.

The parameter known as recurrence rate, RR, is a measure of the tendency of a system to return nearby to a previous state. RR is calculated as the percentage of recurrence points in the recurrence plot and, therefore, it depends on the value of the threshold ε. Though nonlinear, the dependence of RR on ε usually presents a linearly scaling region, within which it is appropriate to search for an optimal value of the threshold.

The determinism DET is the statistical quantification of the predictability of a system and, in fact, is defined as the ratio of the recurrence points aligned along diagonals parallel to the main diagonal, LOI, to the entire set of recurrent points.

In a similar fashion, the parameter laminarity LAM evaluate the number of points lying on vertical (or horizontal) lines, which are due to the permanence of the system in a given dynamical state for a time corresponding to the number of aligned points in the RP.

The mean and values of the lengths of diagonal lines and of vertical lines are respectively expressed by L, predictability time of the system, and TT, trapping time, i.e. the mean time scale (in terms of sampling intervals) for which small changes are observed in time series. Another relevant parameter is the divergence DIV, i.e. the inverse of the maximum length of diagonal lines in the plot.

The mean period of the dynamics of the system has been related in [7, 14] with the parameter defined as recurrence of the first kind, T_1, calculated as the average of empty space between the points of the RP. Taking this value as a reference, it is possible to calculate the probability distributions of periods t separating the diagonal lines and, also, the recurrence period density entropy, $ENTR_t$. Both the latter parameters, T_1 and $ENTR_t$, might be of particular interest when the system may express a variety of periodic behaviours, such as when bifurcations as period doubling and intermittency are expected.

5. Results and discussion

This section reports the results of the analyses performed on the time series of the temperature at point N in the scheme in figure 1, for a set of simulations that have been chosen as representative of the solutions found for increasing values of the Rayleigh number in the period doubling route to chaos. The cases considered are summarized in Table 1. Parenthetically, for the sake of comparisons, such solutions are the same discussed in [3–5].

In accordance with the methodological guidelines described in the previous section, the embedding dimension for the reconstruction of the phase space has been set to 1 (i.e. no embedding has been considered). The choice of the radius threshold, ε, has been performed on the basis of the sensitivity analysis on parameters RR and DET for the solution P_{32} at $Ra = 1.94975 \times 10^5$. figure 2 (a) and (b) reports the values of the two parameters for increasing ε; both show the existence of a scaling region and allow to justify the choice of an optimal threshold corresponding to $\varepsilon = 0.03$.

Figure 3 (a)-(d) and figure 4 report the temperature time series and the RPs for the cases P_1, QP, P_2, P_4 and P_8. The RPs for the higher order periodic solutions, up to P_{128}, have been

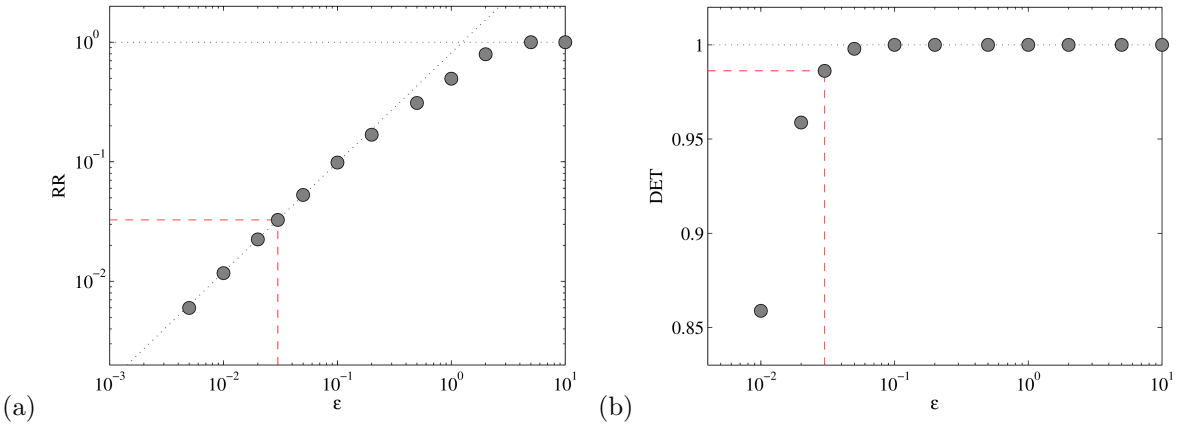

Figure 2. Plots of recurrence rate RR and determinism DET as a function of threshold ε for $Ra = 1.94975 \times 10^5$ (P_{32} regime). Statistics are computed on a sequence of 50000 samples ($\Delta t = 3.3 \times 10^{-2}$) of the normalized temperature series, with embedding dimension and time delay set to $m = 1$ and $\tau = 1$, respectively. The chosen threshold value $\varepsilon = 0.03$ is highlighted in the plots.

calculated but are not reported for the sake of brevity. For each of the periodic solutions in figure 3 (a), (c), (d) and figure 4, the pattern that corresponds to a complete limit cycle in phase space has been encircled and, in fact, it is possible to observe its identical repetition along the main diagonal of the RP.

Such a behaviour cannot be observed in figure 3 (b), as a consequence of the quasiperiodic dynamics of the time series, giving rise to a trajectory in phase space that continuously whirls on a T_2 torus but never closes on it. Moreover, it is possible to observe that the patterns in the RP of the quasiperiodic case can be considered as originated by a sort of weak modulation of the basic sub-patterns that correspond to the two modes of the P_2 solution; in fact, such modulation ends as soon as the latter two modes, incommensurate in the quasiperiodic regime, lock together in the P_2 limit cycle. More details corroborating this observation are reported in [3–5].

Table 1. *Ra*-values and corresponding flow regimes analysed in the present work.

flow regime		$Ra \times 10^{-5}$
periodic	P_1	1.71
quasiperiodic	QP	1.76875
periodic	P_2	1.8
periodic	P_4	1.93645
periodic	P_8	1.945
periodic	P_{16}	1.94925
periodic	P_{32}	1.94975
periodic	P_{64}	1.95
periodic	P_{128}	1.95008
incipient chaos	CH_1	1.955
fully-developed chaos	CH_2	2

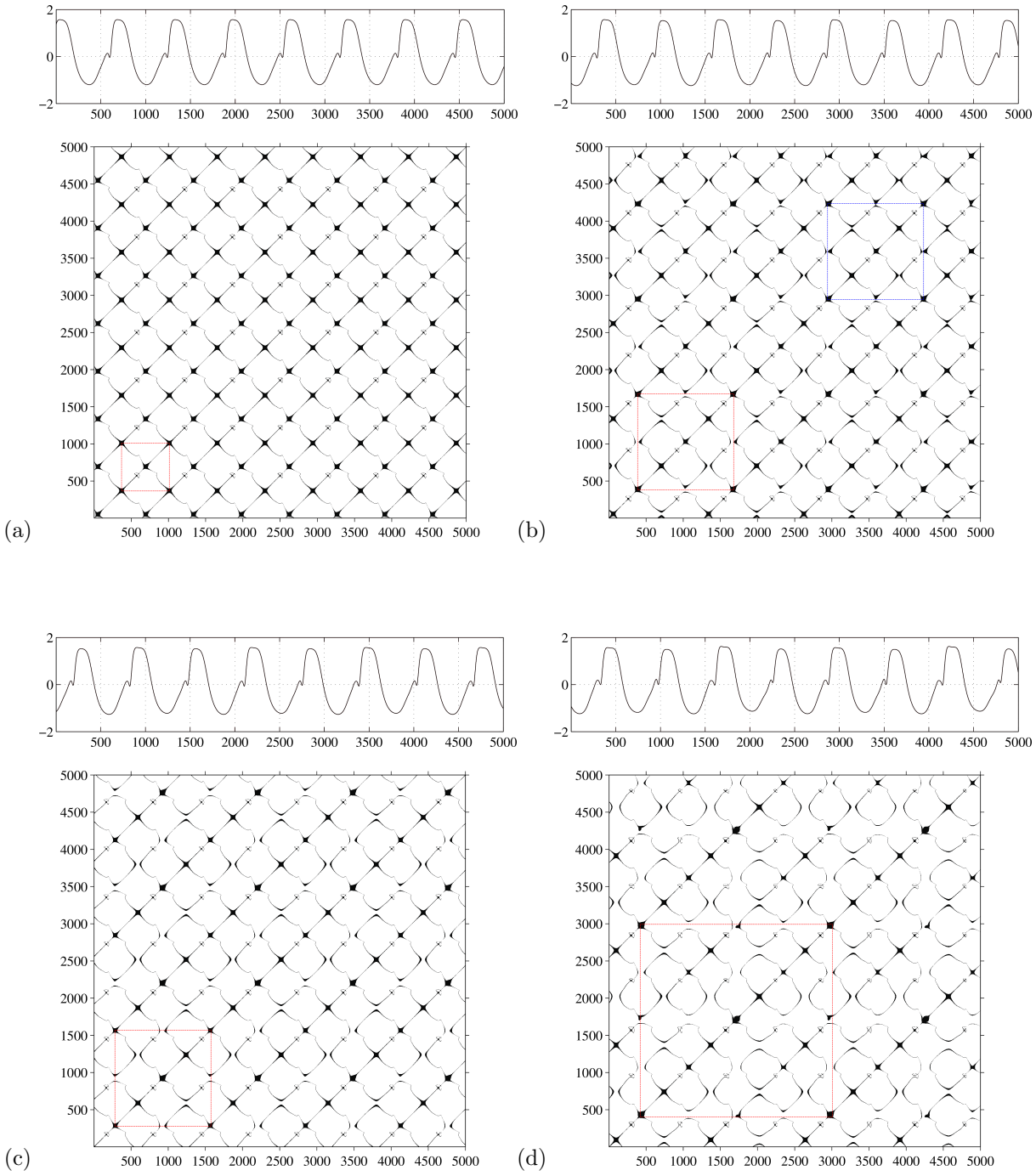

Figure 3. Normalized temperature time series and corresponding recurrence plot for regimes (a) P_1, (b) QP, (c) P_2, (d) P_4. Plots have been obtained on a sequence of 5000 samples ($\Delta t = 3.3 \times 10^{-2}$) with embedding dimension $m = 1$, time delay $\tau = 1$ and threshold $\varepsilon = 0.03$. Recurrent patterns for each regime are framed in red, except for plot (b), where two analogous but slightly different patterns are highlighted with red and blue frames.

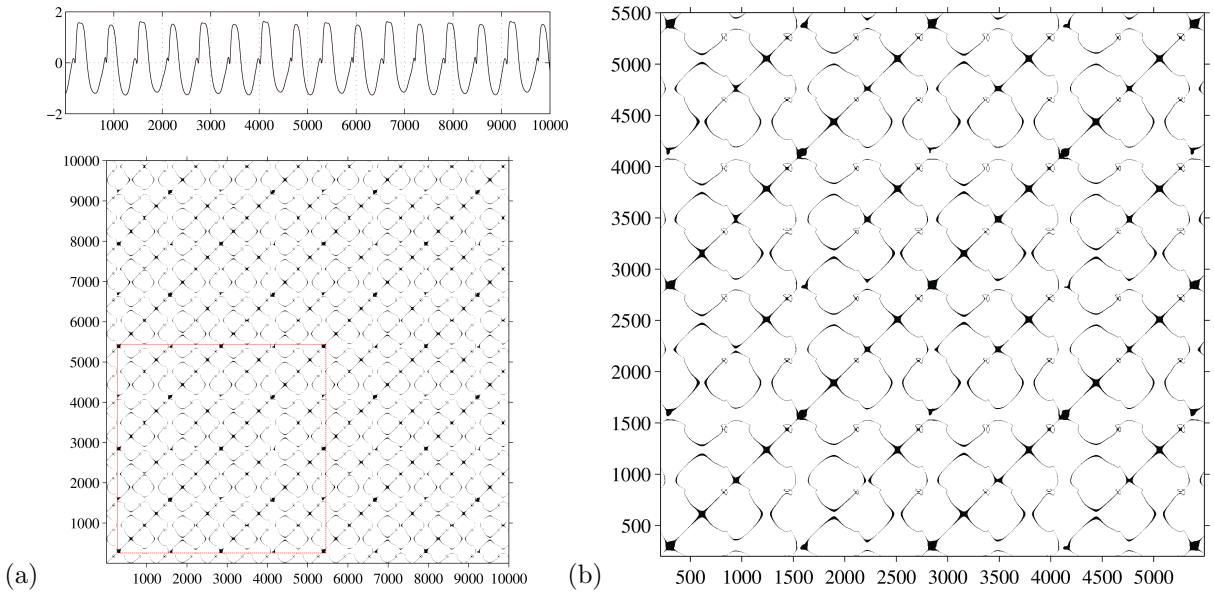

Figure 4. Normalized temperature time series and corresponding recurrence plot (a) for regime P_8, alongside with a zoomed view (b) of the recurrent pattern. The plot has been obtained on a sequence of 5000 samples ($\Delta t = 3.3 \times 10^{-2}$) with embedding dimension $m = 1$, time delay $\tau = 1$ and threshold $\varepsilon = 0.03$.

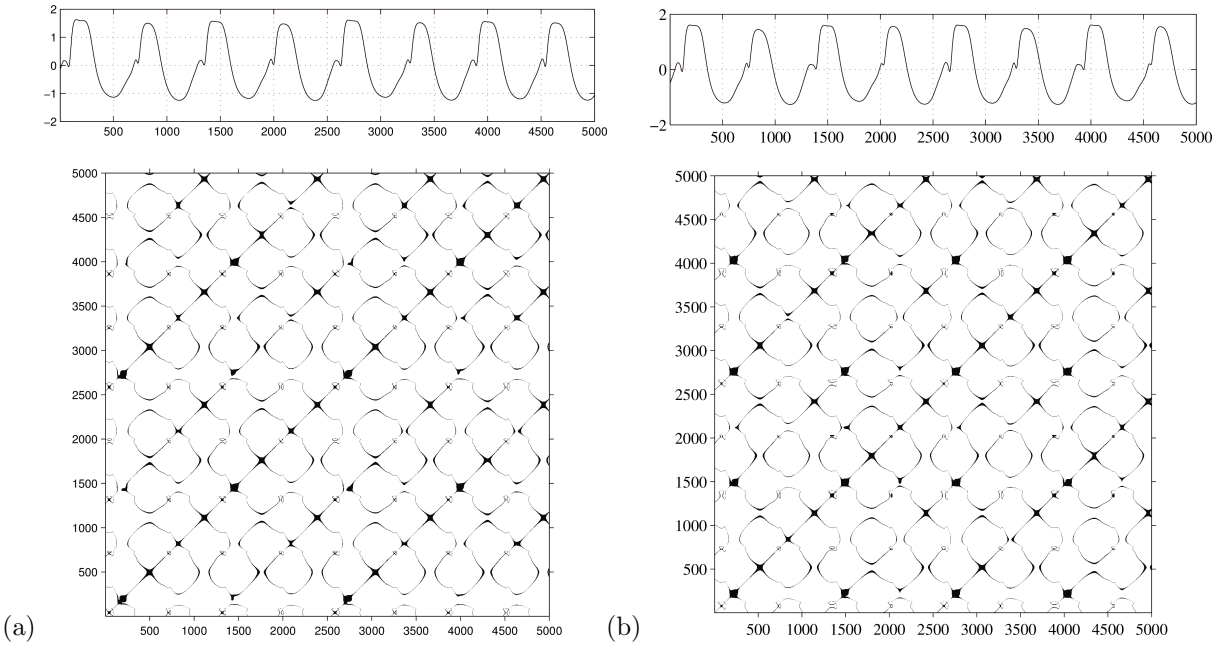

Figure 5. Normalized temperature time series and corresponding recurrence plot for regimes (a) CH_1 and (b) CH_2. The plots have been obtained on a sequence of 5000 samples ($\Delta t = 3.3 \times 10^{-2}$) with embedding dimension $m = 1$, time delay $\tau = 1$ and threshold $\varepsilon = 0.03$.

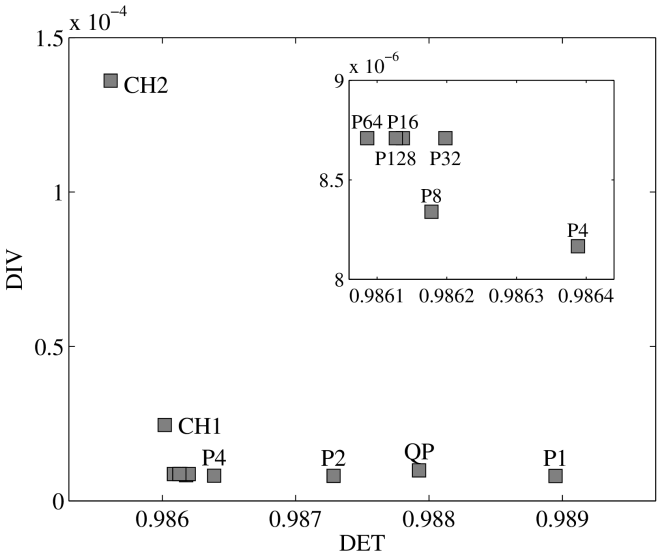

Figure 6. Plots of divergence DIV against determinism DET for all the regimes considered here. Statistics are computed on sequences of 50000 samples ($\Delta t = 3.3 \times 10^{-2}$) of the normalized temperature series, with embedding dimension and time delay set to $m = 1$ and $\tau = 1$, and with a threshold value $\varepsilon = 0.03$.

It is worth observing that, as a consequence of the period doubling from P_1 to P_2, the first single pattern in figure 3 (a) is doubled in a couple of different sub-patterns in figure 3 (c); the same observation can be drawn for the following period doublings, from P_2 to P_4 and from P_4 to P_8, each corresponding to a duplication in the high order dynamics of the basic sub-patterns observable in the low order one, with progressively smaller differences among them. Such a behaviour has been identically observed also for the higher order period doublings, not reported here. This progression clearly determines a rapid growth of the complexity of the RP global structure and, as it is typical in a period doubling cascade, ends with the appearance of chaotic dynamics.

In fact, figure 5 (a) and (b), report the RPs for two chaotic solutions. In particular, they are representative of the case of incipient chaos at $Ra = 1.955 \times 10^5$ and of developed chaos at $Ra = 2 \times 10^5$, respectively. From the observation of these plots, it is easy to identify the growing influence of chaotic mixing on the complexity of the RP structure, that can be recognised in the higher variety and in the lack of repeatability of the basic patterns.

Reported discussion on the topology of the RPs show that recurrence analysis represents a powerful tool for the characterisation of bifurcation path such as the period doubling cascade discussed in the present study. Therefore, the interest of the study has been extended to the extraction of the RQA statistical parameters discussed in the previous section.

All of the parameters previously mentioned have been evaluated for the entire set of simulations along the period doubling cascade. From their preliminary analysis, it has emerged that not all of the parameters are useful for the dynamics under consideration in the present study. For this reason, and for the sake of conciseness, a different approach has been chosen here. In particular, each of the analysed simulations has been described by means of the couple of parameters (DET, DIV), i.e. those showing the highest sensitivity, and are reported in the parameter space in figure 6.

The separation in the chosen parameter space between periodic and chaotic solutions is evident; this is true both for the case CH_1, corresponding to incipient chaos, and, markedly

more, for the case CH_2. These results demonstrate the capabilities and flexibility of RPs and of RQA in the characterisation of transitional phenomena in nonlinear dynamics and will be used in the extension of the present study to the analysis of the more complex dynamics observed in [2] for a cavity aspect ratio $A = 5$.

6. Concluding remarks

The suitability and applicability of Recurrence Analysis to the identification of successive flow bifurcations of a natural convection flow from an enclosed horizontal cylinder was investigated here. In the case under consideration, the scenario leading to chaos consists in a sequence of period-doubling bifurcations, preceeded by a window of quasiperiodic flow. The analyses benefitted of the existence of an extensive database of numerical simulations already described and discussed in recent works.

First, an optimal value of the threshold ε for the identification of recurrence points was sought for and identified on the basis of a single case. Successively, recurrence plots were carried out for a set of simulated time series, corresponding to the different regimes encountered throughout the route to chaos. A clear distinction between the regimes could be easily assessed by visual inspection of the plots. The features of period-doublings were clearly displayed, as well as the mixing characteristics of deterministic chaos.

Secondly, recurrence quantification analysis tools revealed that some of the most relevant statistics computed on recurrence plots allowed for a rather simple discrimination between periodic and chaotic solutions.

It is concluded that recurrence analysis is indeed a powerful tool for the characterisation of transitional dynamics in buoyancy-induced flows. Further application of the technique on more complex scenarios occurring on the same case (but for different values of the system main parameters) is thus envisaged.

Acknowledgments

The authors wish to acknowledge the use of the software "CRP toolbox" and to thank the Authors who provided it at `http://tocsy.pik-potsdam.de/CRPtoolbox`.

References

[1] Yang K T 1988 *J. Heat. Transf.* **110** 1191–1204
[2] Angeli D, Pagano A, Corticelli M A, Fichera A and Barozzi G S 2011 *Front. Heat Mass Transf.* **2** 023003
[3] Angeli D and Pagano A 2013 *Int. J. Therm. Sci.* **68** 20–31
[4] Pagano A and Angeli D 2016 *Int. J. Therm. Sci.* **99** 195–203
[5] Angeli D and Pagano A 2016 *Int. J. Therm. Sci.* **109** 231–241
[6] Kuznetsov Y 1998 *Elements of Applied Bifurcation Theory* 2nd ed (*Applied Mathematical Sciences* vol 112) (New York: Springer-Verlag)
[7] Marwan N, Romano M, Thiel M and Kurths J 2007 *Physics Reports* **438** 237–329
[8] Angeli D, Levoni P and Barozzi G S 2008 *Int. J. Heat Mass Transf.* **51** 553–565
[9] Gresho P M 1990 *Int. J. Num. Meth. Fluids* **11** 587–620
[10] Barozzi G S, Bussi C and Corticelli M A 2004 *Num. Heat Transf. B* **46** 56–77
[11] March T, Chapman S and Dendy R 2005 *Physica D* **200** 171–184
[12] Webber C and Zbilut J 2005 *Tutorials in Contemporary Nonlinear Methods for the Behavioral Sciences* ed Riley M and Van Orden G pp 26–94
[13] Marwan N 2011 *Int. J. Bifurcat. Chaos* **21** 1003–1017
[14] Thiel M, Romano M and Kurths J 2004 *Phys. Lett. A* **330** 343–349